# Biological Effects of High-Energy Neutrons Measured In Vivo Using a Vertebrate Model

Authors: Kuhne, Wendy W., Gersey, Brad B., Wilkins, Richard, Wu, Honglu, Wender, Stephen A., et al.

Source: Radiation Research, 172(4) : 473-480

Published By: Radiation Research Society

URL: https://doi.org/10.1667/RR1556.1

RADIATION RESEARCH **172**, 473–480 (2009)
0033-7587/09 $15.00

DOI: 10.1667/RR1556.1

# Biological Effects of High-Energy Neutrons Measured *In Vivo* Using a Vertebrate Model

Wendy W. Kuhne,[a,1] Brad B. Gersey,[c] Richard Wilkins,[c] Honglu Wu,[d] Stephen A. Wender,[e] Varghese George[b] and William S. Dynan[a]

[a] *Institute of Molecular Medicine and Genetics;* [b] *Department of Biostatistics, Medical College of Georgia, Augusta, Georgia;* [c] *Center for Applied Radiation Research, Prairie View A&M University, Prairie View, Texas;* [d] *Human Adaptation and Countermeasures Division, NASA Johnson Space Center, Houston, Texas; and* [e] *Los Alamos Neutron Science Center, Los Alamos National Laboratory, Los Alamos, New Mexico*

**Kuhne, W. W., Gersey, B. B., Wilkins, R., Wu, H., Wender, S. A., George, V. and Dynan, W. S. Biological Effects of High-Energy Neutrons Measured *In Vivo* Using a Vertebrate Model. *Radiat. Res.* 172, 473–480 (2009).**

**Interaction of solar protons and galactic cosmic radiation with the atmosphere and other materials produces high-energy secondary neutrons from below 1 to 1000 MeV and higher. Although secondary neutrons may provide an appreciable component of the radiation dose equivalent received by space and high-altitude air travelers, the biological effects remain poorly defined, particularly *in vivo* in intact organisms. Here we describe the acute response of Japanese medaka (*Oryzias latipes*) embryos to a beam of high-energy spallation neutrons that mimics the energy spectrum of secondary neutrons encountered aboard spacecraft and high-altitude aircraft. To determine RBE, embryos were exposed to 0–0.5 Gy of high-energy neutron radiation or 0–15 Gy of reference γ radiation. The radiation response was measured by imaging apoptotic cells *in situ* in defined volumes of the embryo, an assay that provides a quantifiable, linear dose response. The slope of the dose response in the developing head, relative to reference γ radiation, indicates an RBE of 24.9 (95% CI 13.6–40.7). A higher RBE of 48.1 (95% CI 30.0–66.4) was obtained based on overall survival. A separate analysis of apoptosis in muscle showed an overall nonlinear response, with the greatest effects at doses of less than 0.3 Gy. Results of this experiment indicate that medaka are a useful model for investigating biological damage associated with high-energy neutron exposure.** 

## INTRODUCTION

Understanding the biological effects of high-energy neutrons is important because humans live and work in aerospace radiation environments, even if only temporarily. Galactic cosmic radiation (GCR) and solar particle radiation have high-energy components that can interact with nuclei in the atmosphere and aerospace vehicle structures to produce high-energy secondary neutrons (*1*). These neutrons have a broad energy spectrum ranging from below 1 to over 1000 MeV (*2*). High-energy and relativistic neutrons interact with matter primarily through elastic and inelastic collisions with nuclei. As a result of these types of interactions, secondary particles are produced, which may include charged particles, neutrons and γ rays. Both primary and secondary neutrons have the ability to penetrate great distances through matter before transferring their kinetic energy. Severe localized damage may occur if the kinetic energy transfer site is located in tissue (*3*).

Relative biological effectiveness (RBE) is used for establishing radiation risk and protection criteria. Prior estimates of RBE for neutrons have been determined from atomic bomb survivor data, from animal experiments using life expectancy, solid cancer mortality, tissue-specific cancer incidence, DNA damage and mutations, and from *in vitro* cellular transformation rates (*4–9*). Results are based primarily on experiments with exposures to neutron energies below 10 MeV. There has been only one prior direct measurement of RBE of high-energy neutrons (*10*); it was performed in a ground-based experiment at the Los Alamos Neutron Science Center (LANSCE)/Weapons Neutron Research (WNR). The high-energy neutron spectrum (Fig. 1A) (*11*) delivered at LANSCE/WNR is similar in shape and energy range to the secondary neutron energy spectrum found aboard the Space Shuttle and the ISS (*12*). The RBE, 16.4 ± 1.4, was determined using an end point of micronucleus formation in human cultured fibroblast cells (*10*).

To make radiation biology studies at LANSCE/WNR more relevant to human radiation protection, it is important to extend high-energy neutron studies to intact organisms, which respond to radiation injury not only at the cell and molecular levels but also at the tissue and organismal levels. Here we report results obtained at the LANSCE/WNR high-energy neutron source using intact vertebrate Japanese medaka fish embryos (*Oryzias latipes*). To our knowledge, this is the first study of

[1] Address for correspondence: Medical College of Georgia, IMMAG CA-3053, Augusta, GA 30912; e-mail: wkuhne@mcg.edu.

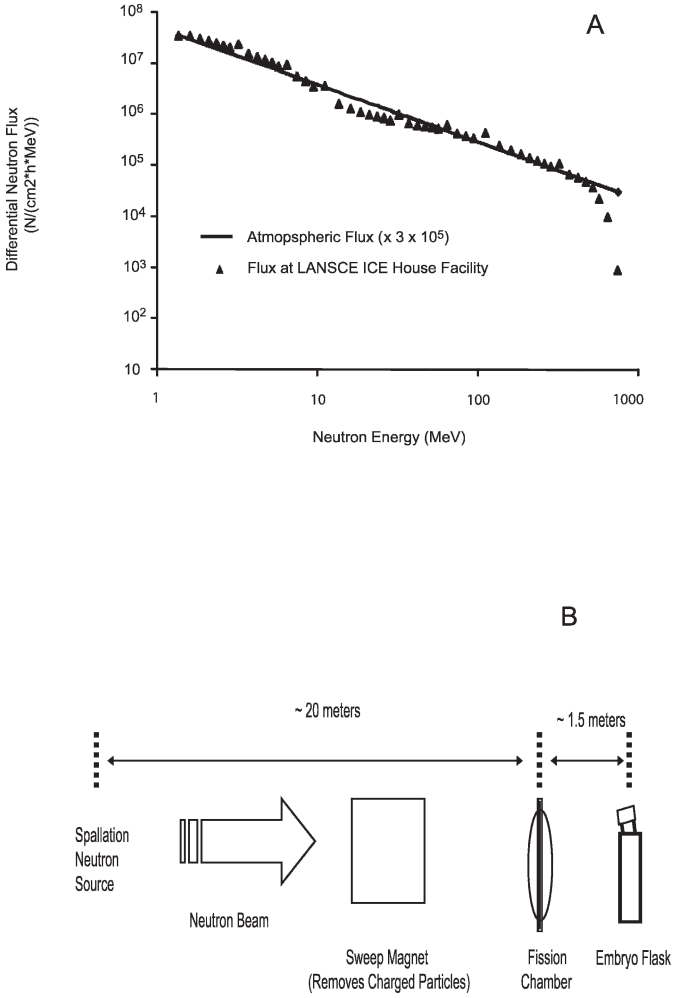


**FIG. 1.** Panel A: Differential energy spectrum of the LANSCE/WNR neutron beam line used in this study, and neutron flux found at an altitude of 12,000 m in the atmosphere. Panel B: Medaka irradiation using the 30L LANSCE/WNR neutron beam line. Relative positions of the neutron source, sweep magnet, fission chamber and embryo flask are shown (figure is not to scale). In some experiments, a TEPC was placed in line behind the embryo flask for dosimetry purposes.

an intact vertebrate using neutrons with this range of energies. As a model organism, the medaka has several strengths, including a fully sequenced genome that contains orthologs of most or all mammalian DNA damage surveillance and repair genes (*13*). Medaka also have a full complement of vertebrate-specific organs of radiobiological interest, including a brain, eyes, spinal cord, vasculature, and digestive, excretory and hematopoietic systems (*14–16*). Medaka have been used extensively in prior radiation studies. Spontaneous and γ-ray-induced mutation rates are similar to those reported in mice (*17, 18*). Medaka have been used to estimate RBEs for HZE-particle radiation based on mutation end points (*19*) and in a space-flight experiment to investigate effects of microgravity on the vertebrate life cycle, with hatching rates, development and fertility of offspring as end points (*20*). Medaka are a robust species and are more resistant than other vertebrate models to temperature fluctuations, physical disturbances and changes in light cycles, which are inherent in beam-line experiments and have the potential to mask or bias radiation responses (*15*).

In the present study, we investigated overall survival and apoptosis in the muscle tissue, brain and eyes of the developing embryo. Effects on the brain are important because neurogenesis defects underlie the behavioral and cognitive effects of radiation exposure. Prior studies in zebrafish embryos show that radiation-induced apoptosis in the central nervous system is a quantifiable end point that exhibits a linear, no-threshold response (*21*). Moreover, apoptosis reflects a p53-dependent DNA damage response, making it a surrogate measure of radiation-induced damage to the genetic material (*22, 23*).

## MATERIALS AND METHODS

### *Production and Transport of Medaka Embryos*

Experiments were carried out using CAB strain medaka embryos produced by a colony at the Medical College of Georgia. Protocols were approved by the Institutional Animal Care and Use Committees at the Medical College of Georgia and Los Alamos National Laboratory (LANL). The Medical College of Georgia is accredited by the Association for Assessment and Accreditation of Laboratory Animal Care International and the United States Department of Agriculture. Embryos were obtained from adult breeding pairs maintained at 27 ± 1°C with a diurnal cycle of 14 h light and 10 h dark. Fertilized eggs were collected 1 h after initiation of the light phase of the cycle. Eggs were inspected to confirm fertilization and staged using standard criteria (*16*). Embryos were shipped overnight at ambient temperature to and from LANL. Water quality parameters of pH (7.5–8.3), conductivity (500–560 μS), temperature (22–24°C), alkalinity (80–100 mg/liter as $CaCO_3$), hardness (100–120 mg/liter as $CaCO_3$), and dissolved oxygen (4–6 mg/liter) were checked before and after shipping.

### *Neutron Radiation and Measurement*

Controlled exposures to high-energy neutrons were conducted at the high-energy neutron source at the Los Alamos Neutron Science Center (LANSCE), Los Alamos National Laboratory, Los Alamos, NM. Exposures were performed in the Irradiation of Chips and Electronics (ICE House) located 30 degrees left (30L) of the axis of the incident proton beam. Spallation neutrons were generated by an 800 MeV pulsed proton beam incident on a tungsten target (*24*). After generation, the neutrons pass by a sweep magnet, which removes charged particles. The neutrons then pass through a fission chamber, which is used to measure the neutron fluence, and time-of-flight techniques are used to measure absolute neutron intensities and the neutron energy spectra, as shown in Fig. 1B (*25*). Dosimetry was performed using a tissue-equivalent proportional counter (TEPC) (*26*). The TEPC used in this experiment is functionally identical to the one used aboard the space shuttle. Previous microdosimetry measurements taken on the beamline, measuring the absorbed dose, along with the time-of-flight information showed a differential energy neutron spread ranging from 1 to 800 MeV (*27*). Embryos were exposed to the neutron beam in liquid-filled T-25 polystyrene flasks containing a maximum of 60 embryos in water containing 0.0001% methylene blue. The experimental setup, shown in Fig. 1B, illustrates that the flasks were placed in the center of the neutron beam with a

minimum of intervening material upstream of the flasks. The small amount of intervening material upstream was insufficient to produce changes in the neutron beam energy or secondary charged-particle buildup. Stage 27 (24 somite stage) embryos were irradiated at 24 ± 2°C for various times to deliver the desired total absorbed doses. A dose rate of 12 mGy $h^{-1}$ was used for the survival assay and a dose rate of 15 mGy $h^{-1}$ for investigation of acute effects arising in the form of DNA damage using the TUNEL assay.

### *Gamma-Ray Exposure and Measurement*

Medaka embryos were exposed to γ rays at the Medical College of Georgia using a calibrated $^{137}Cs$ source (J. L. Shepherd, Mark I 68A, San Fernando, CA) at a dose rate of 0.0137 Gy $min^{-1}$ (822 mGy $h^{-1}$), which is the lowest dose rate possible for this source. Embryos exposed to the reference γ-ray source were at the same developmental stage as the embryos used at LANL and were subsequently exposed to simulated shipping conditions to ensure comparability of the results. Gamma-ray dose rate was confirmed using thermoluminescence dosimeters (Landauer Inc., Glenwood, IL).

### *Survival Assays*

A minimum of 30 embryos were irradiated with varying doses and maintained at 24 ± 1°C in water containing 0.0001% methylene blue until hatching. After hatching, embryos were observed for 10 days and total mortality was recorded at the end of the observation period. A dose–response curve for percentage survival was fitted with a linear regression to determine the $LD_{50}$.

### *Whole-Mount TUNEL Assay*

After irradiation, embryos were maintained at 24 ± 1°C for 30 h, fixed and subjected to a fluorescence *in situ* terminal deoxynucleotidyl transferase-mediated dUTP nick-end labeling (TUNEL) assay to detect DNA fragmentation, which is characteristic of apoptotic cells (Chemicon, International, Inc., Temecula, CA) (*21*). They were stained with rhodamine-labeled anti-digoxigenin Fab fragment (Roche Applied Science, Indianapolis, IN) and cleared with benzyl amino benzoate immediately prior to imaging to promote uniform detection of staining throughout the depth of the embryo (*28*). Confocal images were collected using a Zeiss LSM 510META confocal laser scanning microscope with an Achroplan 20× water objective (Carl Zeiss Inc., Thornwood, NY). The rhodamine fluorophore was excited using 543 nm He:Ne laser illumination, and confocal images were collected using a 3-μm step size. Approximately 100 optical slices of the tail and 150 optical slices of the head were collected for each embryo. Three-dimensional renderings of the Z-stack images were created and analyzed for the presence of TUNEL-positive cells as described (*21*) using Volocity 3D imaging software (Version 4.2.0 Improvision, Lexington, MA).

### *Statistical Analysis*

The data set was checked for normality and outliers. We used three statistical tests for detection of outliers in the regression analyses of the dose–response relationship: (1) Cook's D test, which measures the effects on slope, (2) DEFITS, which measures the effects on predicted response, and (3) COVARATIO, which measures the effects on the variance-covariance matrix (*29*). One observation from the neutron data and one from the γ-ray data were highly influential outliers by all three criteria and were excluded from analyses. RBE, the parameter of interest, is defined as the ratio of two slopes: that of the dose response to secondary neutron exposure and that of the dose response to the reference γ radiation. Bootstrapping, a data-based simulation method (*30*), was used to generate slopes and their ratios and to calculate 95% CI of RBE for the tail and head data. Bootstrapping is a computationally intense approach to estimation using the empirical distribution of the observed data rather than assuming that the data follow a particular distribution. Bootstrapping was performed by constructing a large number of repeated samples from the observer data using valid resampling techniques (*30*). We generated 10,000 repeated samples and constructed 10,000 values of RBE. The end points of the 95% CI are estimated as the 2.5th and 97.5th percentiles of the ordered values of these RBEs. We also determined the confidence intervals analytically, assuming that the ratio estimator is approximately normally distributed and employing the Taylor series approximation (also known as the delta method) to estimate the standard error of *R*. All analyses were performed using SAS statistical software (SAS, Cary, NC).

## RESULTS

### *Dose Response Measured using a Survival End Point*

Embryos were irradiated with neutrons or γ rays as described in the Materials and Methods. Embryos were held until 10 days after hatching (20 days postirradiation), and survival was scored based on the fraction of embryos that were alive. Survival was 80–100% for nonirradiated embryos and declined with increasing dose of neutrons or γ rays (Fig. 2). Data were fitted to a linear model by regression analysis and resulted in $LD_{50/20}$ values of 0.53 Gy for neutrons and 25.7 Gy for γ rays. The calculation of the slopes and the 95% CI were calculated using the Taylor series approximation. The ratio of the slopes of the survival curves for neutrons and γ rays provided an RBE of 48.1 (95% CI 30.0–66.4) (Fig. 2).

### *Dose Response Measured using an End Point of Apoptosis in Embryo Heads*

TUNEL staining was performed to label apoptotic cells *in situ* within the irradiated embryos and three-dimensional image data were collected by confocal microscopy. Embryos were fixed and imaged at stage 30, when the brain was completely formed, migration of neuronal cells had formed gray matter, and melanization of the eye was nearly complete. Cleared embryos were positioned with the dorsal side toward the objective, and optical slices were collected from the top of the head to the bottom of the jaw (Fig. 3). A three-dimensional model was constructed from the confocal image stack using Volocity software. TUNEL-stained cells were then classified and counted. A region of strong autofluorescence between the eyes and optic tectum, near the center of the head, was excluded from the analysis. At least seven embryos were analyzed per radiation dose. The slope of the dose–response curve was determined by linear regression (Fig. 4). Values for slopes, RBE and confidence intervals are given in Table 1. The calculated RBE of 24.9 is a factor of two lower than the RBE from the survival data. Confidence intervals are reported in Table 1 both for the bootstrap and the normal theory methods. The confidence intervals determined by the two methods are similar. Because of the potential violations of underlying assumptions of the normal

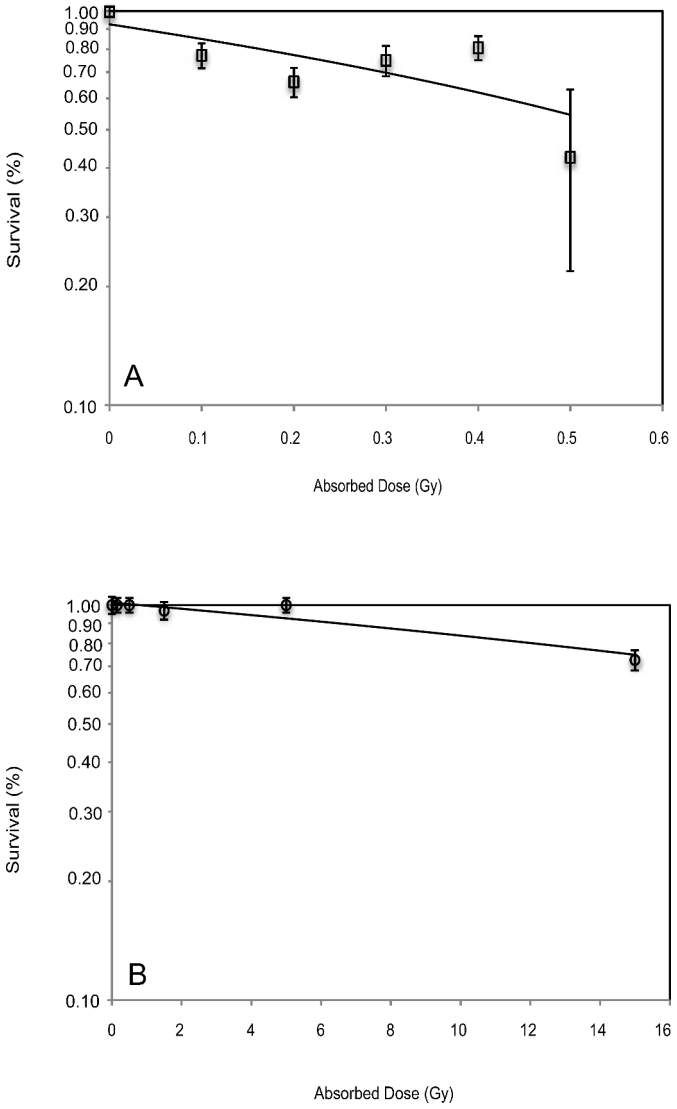


**FIG. 2.** Survival curves for embryos exposed to high-energy neutrons and γ rays. Embryos were evaluated at 10 days after hatching as described in the Materials and Methods. Percentage survival was calculated as the number of surviving embryos in each group relative to the number of embryos at the start of the experiment. The number of embryos used was based on logistical constraints at the LANL site and was a minimum of 30 per dose. The $R^2$ values, 0.63 for neutrons and 0.72 for γ rays, were determined by linear regression. Panel A: The dose response of the embryos irradiated with neutrons. Panel B: The dose response of embryos exposed to γ rays.

theory method, however, the confidence intervals determined by the bootstrap method are expected to be more accurate (*31*).

### *Comparison with Embryo Tails*

To analyze the radiation response in a different tissue type, we also analyzed a region of the tail. At stage 30, the tail is composed primarily of developing muscle tissue. Cells are rapidly dividing as the tail grows in mass and length. Confocal images were collected laterally or dorsally, depending on the natural position of the tail. A three-dimensional model was again constructed for each embryo based on the confocal image stack and TUNEL-positive cells were counted in a region of interest extending from the tip of the spine rostrally for 500 μm. Dose–response curves are shown in Fig. 5. For gamma-ray exposure, the response was linear, as in the heads. For neutrons, the response increased roughly linearly with dose through 0.3 Gy but declined at the highest dose of 0.5 Gy. The overall neutron dose response required a second-order polynomial model to obtain a satisfactory fit to the observed data, and the RBE for the data was, by definition, indeterminate. It was possible, however, to fit a subset of the data from 0–0.3 Gy to a linear model, with a nominal RBE of 147 (95% CI 29–138) (Table 1). The mechanism responsible for the nonlinear response is uncertain and might be attributable to clearance of apoptotic cells from the rapidly proliferating muscle tissue. Because of the low dose rate delivered by the neutron beam, a 0.5-Gy exposure required ~37 h, significantly extending the total time elapsed from the beginning of the exposure to the time of fixation (67 h for 0.5 Gy compared to 36 h for 0.1 Gy). It may be that during this time apoptotic cells have been lost for analysis.

## DISCUSSION

We have measured the biological effects of exposure to a broad spectrum of high-energy neutrons in a medaka embryo model. The energy spectrum used in this ground-based experiment spanned the range of 1 to 800 MeV and resembles the energy spectrum in the upper atmosphere. A linear dose response was observed both for overall survival and for induction of apoptosis in cells of the developing brain. The linearity of the response allowed calculation of an RBE of 25–48 relative to γ radiation. It was not possible to calculate an RBE based on apoptosis in rapidly growing muscle tissue because of this nonlinear response, although analysis of a low-dose subset of the data indicated that this tissue is probably also very sensitive to neutrons. Although an RBE has been reported previously for human fibroblasts exposed to the same high-energy neutron source, the present studies are, to our knowledge, the first to report an RBE for an intact vertebrate organism.

The 95% confidence intervals for the RBE values, estimated by bootstrapping or Taylor series approximation, spanned a twofold range above and below the measured RBE. The breadth of the interval reflects high interindividual variability and may be attributable to the complexity of the *in vivo* response, which reflects events not only at the cellular and molecular levels but also at the tissue and organismal levels. It is also possible that there was genetic heterogeneity, because the experiments were performed using an outbred population.

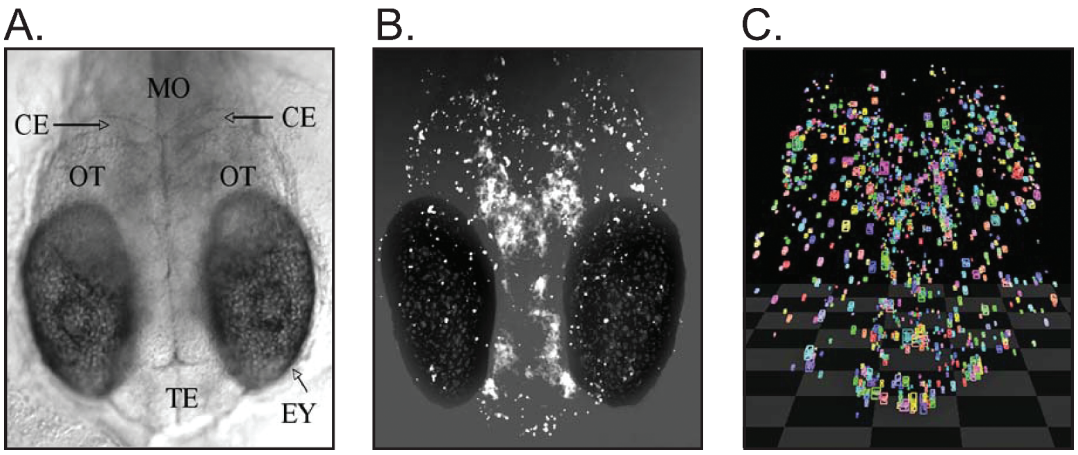


**FIG. 3.** Representative images of structures and apoptotic cells in embryo head. Embryos are oriented with the dorsal side facing the microscope objective. Panel A: Unirradiated uncleared embryo showing anatomical features of the central nervous system. CE = cerebellum; EY = eye; OT = optic tectum; TE = telencephalon. Panel B: Optical section of a representative medaka embryo exposed to 0.1 Gy of neutrons and stained by a TUNEL procedure. White dots indicate TUNEL-positive cells. Note region of diffuse fluorescence at center of brain, which represents TUNEL stain-independent autofluorescence and was excluded from the analysis. Panel C: Three-dimensional rendering of the Z-stack images to illustrate the spatial distribution of TUNEL-positive cells. The figure shows a model created using Volocity Software as described in the Materials and Methods. TUNEL-positive cells were quantified using object classification and counting modules and have been assigned arbitrary colors to aid visualization.

The dose rates for different types of radiation were chosen with the idea that the exposure times required to reach a given end point should be similar; i.e., different types of radiation are ideally delivered at equitoxic rates. The neutron experiments here were performed using the maximum available flux at the LANSCE/WNR facility, which provided a dose rate of 15 mGy $h^{-1}$. The $\gamma$ irradiation was performed using maximum attenuation on the available cesium radiation, which provided a dose rate of 822 mGy $h^{-1}$. Assuming an RBE of about 25, the 55-fold difference in physical dose rate translates to a residual difference in equivalent dose rate of a little over twofold. Moreover, the dose-rate effectiveness factor for neutrons should approximate unity, so that a twofold difference in equivalent dose rate will have no substantial influence on the findings.

There have been two prior studies that reported neutron RBEs for medaka. An RBE of 4.3 ± 0.6 was determined for micronucleus formation in gill cells (*7*), and RBEs of 3–7 were determined for mutations occurring in the male germ line at specific loci (*5, 6*). Both used 1.3 MeV average energy fission neutrons, which are near the bottom end of the range studied here. Data from humans and other vertebrate species provide somewhat higher neutron RBEs. Human data from atomic bomb survivors indicate neutron RBEs of 100 (95% CI 25–400) for solid-cancer mortality (*9*) and 63 (95% CI 0–275) for overall cancer incidence (*8*). A recent review of RBEs for fission neutrons, obtained using a range of model systems and biological end points, reported values of 34–53 for cytogenetic end points in human cell cultures, 3–80 for transformation and genetic end points in mammalian systems, 10–46 for life shortening in mouse models, and 16–59 for tumor induction in specific tissues (*4*). The RBEs measured for high-energy neutrons in the present study are well within these ranges obtained for human and other mammalian species. To our knowledge, there has been only one prior experiment using the LANSCE/WNR broad-spectrum beam to measure an RBE for high-energy neutrons directly. This study reported an RBE of 16.4 ± 1.4 for the induction of micronuclei in human cultured fibroblast cells (*10*).

RBE values are dependent on the type of radiation, the biological end point measured, and the total absorbed dose. A recent study of fast-neutron effects on mouse embryos provides a particularly relevant example, where RBE based on apoptosis in sensitive areas of the eyes or fetal brain of the mouse increased at doses below 1 Gy (*32*). Previous microdosimetry experiments done to characterize the beam line at LANSCE/WNR showed that as the average neutron energy in the beam increases, the measured absorbed dose per incident neutron also increases (*27*). From these results we can conclude that the higher-energy neutrons present in the broad-spectrum neutron beam used in this study can contribute more heavily to the measured absorbed dose than the lower-energy neutrons and could ultimately affect the biological response.

An important question, particularly if RBEs are to be used for regulatory decision making, is the degree to which results in medaka or other non-mammalian models can be extrapolated to humans. The medaka have been shown to display similar rates of mutations to

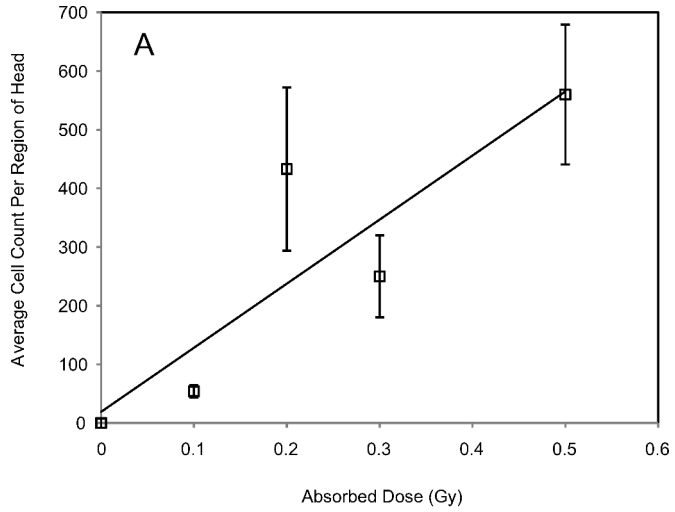


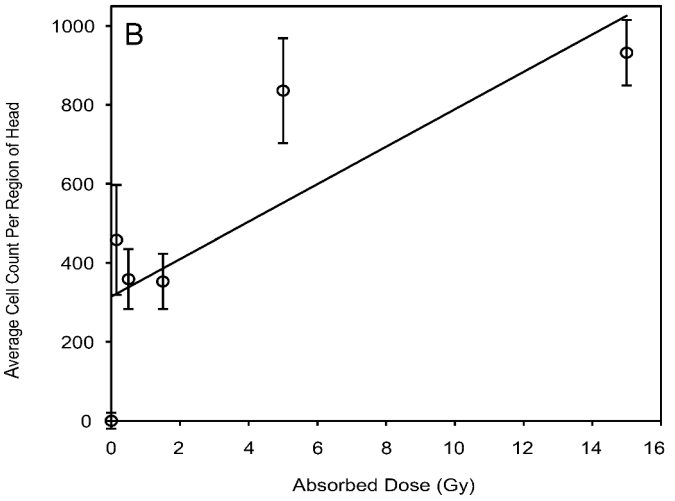


**FIG. 4.** Dose response based on apoptotic cell counts in a defined region of the head including the developing brain and eye. TUNEL-positive cells were imaged by confocal microscopy and scored based on a reconstructed three-dimensional model of the head as shown in Fig. 3. Squares denote high-energy neutron-irradiated samples and circles denote $^{137}$Cs $\gamma$-irradiated samples. Means and standard errors are shown. Trend lines were determined by least-squares regression, with $R^2$ values of 0.77 for neutrons and 0.64 for $\gamma$ rays. Scoring was based on a minimum of seven embryos per group. Panel A: The dose response of the neutron-irradiated samples. Panel B: The dose response of the $\gamma$-irradiated samples.

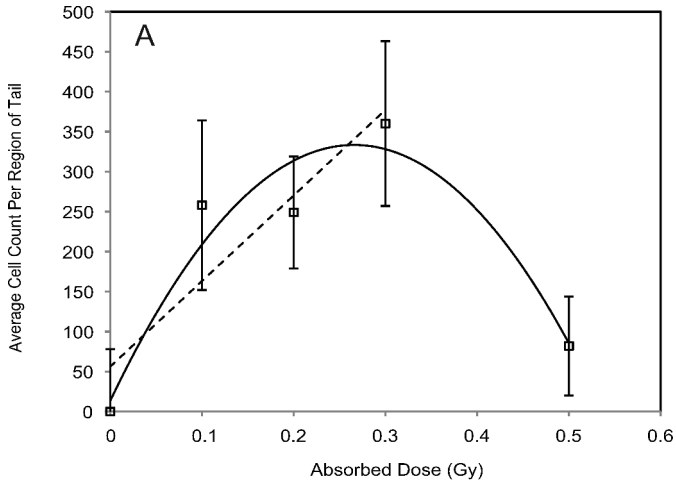


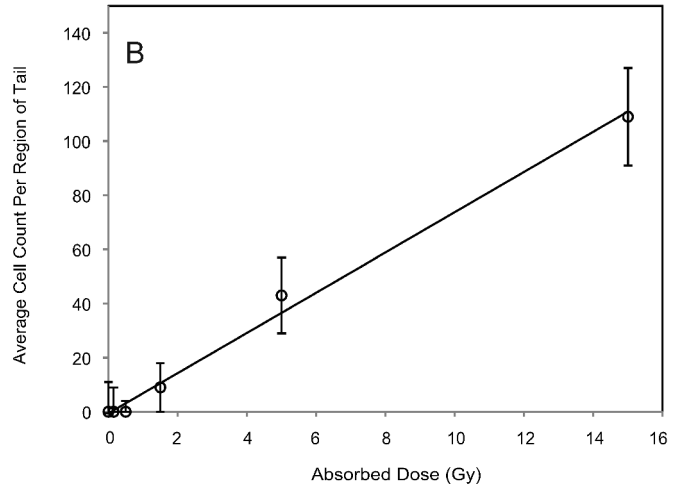


**FIG. 5.** Dose response based on apoptotic cell counts in a defined region of the region of the tail including primarily muscle tissue. TUNEL-positive cells were scored as described in the Materials and Methods. Data are based on a minimum of seven embryos per group. Symbols are as in Fig. 4. Panel A: The dose response of the neutron-irradiated samples. The solid line shows the quadratic model fit to non-linear response of the neutron doses. The dotted line is the linear regression fit to doses up to 0.3 Gy that were used in the calculation of RBE. Panel B: The dose response of the $\gamma$-irradiated samples. The $R^2$ values, 0.82 for neutrons and 0.99 for $\gamma$ rays, were determined by linear regression.

**TABLE 1**
**Results from the Calculation of the Slopes and Ratios of the Slopes for the Neutron and $\gamma$-Ray Exposures Using the Bootstrapping Method**

| | Slope | | | 95% confidence intervals | |
|---|---|---|---|---|---|
| | Neutrons | Gamma rays | Ratio | Bootstrap method | Normal theory method |
| Head | 1088.5 | 43.6 | 24.9 | (13.6, 40.7) | (10.5, 39.3) |
| Tail | 1106.8 | 7.6 | 146.6 | (28.8, 237.9) | (39.3, 253.9) |

exposure to low-LET radiation as those reported in mouse models (*33*). The similarity to mammals in body plan, cell types, tissue architecture and the protein-coding portion of the genome are strengths of medaka as a model organism. Other advantages include (1) the ability to use large numbers of individuals in experiments to increase statistical power, (2) the optically clear chorion and embryo, which facilitate analysis of radiation effects using light microscopy, and (3) a short life span (~2 years) makes it feasible to conduct lifetime studies of radiation effects on tissue degeneration. Clearly, it will be useful to investigate additional end points and to perform studies of adult organisms. Slowly replicating or postmitotic cells of the adult may provide a good model for somatic tissue effects in the human.

## CONCLUSIONS

This experiment represents the first whole-animal biological experiment performed at the LANSCE/WNR ICE House facility. RBEs ranged from 25 for apoptosis in the head of the developing embryo (95% CI 13.6–40.7) to 147 (95% CI 28.8–240) based on a subset of data for the tail. Confidence intervals for apoptosis in the head overlap the only other high-energy neutron RBE of 16.4 ± 1.4, generated at the LANSCE/WNR beam line using cultured human fibroblasts. The confidence intervals for survival overlapped the confidence intervals for apoptosis in the head. The nonlinear response for apoptosis in the tail illustrates the complexity of using intact tissue and tissue-specific responses. Over the past 20 years studies concerning the response of the medaka to ionizing radiation have resulted in a significant body of literature. The results of this experiment indicate that the medaka are useful models for investigating biological damage associated with high-energy neutron exposure. To our knowledge this is the first reported RBE for medaka, or any other intact vertebrate, exposed to high-energy neutrons relevant to the aerospace radiation environment.

## ACKNOWLEDGMENTS

Funding was provided by a grant award from U.S. Department of Energy Low Dose Radiation Research Program (DOE FG02-03ERG3649), a National Research Service Award to Wendy Kuhne (1F32ES015663-01), and a grant award from the National Aeronautics and Space Administration (NCC9-114) to the Center for Applied Radiation Research, Prairie View A&M University. Neutron beam time was supported by the U.S. Department of Energy. We thank Katsuya Miyake and the Medical College of Georgia Cell Imaging Core Facility for assistance with microscopy and data analysis. We thank Li Fang Zhang in the Biostatistics Group at the Medical College of Georgia for her contributions to data analysis. We extend special thanks to Art Bridge at the LANSCE facility and Lingling Ding at the Medical College of Georgia for their assistance with logistical support in this project.

Received: August 7, 2008; accepted: May 20, 2009

## REFERENCES

1. J. W. Wilson, M. S. Clowdsley, F. A. Cucinotta, R. K. Tripathi, J. E. Nearly and G. DeAngelis, Deep space environment for human exploration. *Adv. Space Res*. **34**, 1281–1287 (2004).
2. J. E. Hewitt, L. Hughes, J. W. Baum, A. V. Keuhner, J. B. McCaslin, A. Rindi, A. R. Smith, L. D. Stephens, R. H. Thomas and C. G. Welles, Ames collaborative study of cosmic ray neutrons: Mid-latitude flights. *Health Phys*. **34**, 375–384 (1978).
3. P. Truscott, C. Dyer, H. Evans, A. Sims, C. Peerless, P. Knight, M. Cosby, J. Flatman, C. Comber and N. Hammond, Observations and predictions of secondary neutrons on space shuttle and aircraft. *Adv. Space Res*. **21**, 1707–1716 (1998).
4. NCRP, *The Relative Biological Effectiveness of Radiation of Different Quality*. Report No. 104, National Council on Radiation Protection and Measurements, Bethesda, MD, 1990.
5. A. Shimada, A. Shima, T. Itoh and S. Kondo, Specific-locus mutation frequencies in the medaka, Oryzias latipes: VI, RBE for fission neutrons. *J. Radiat. Res. (Tokyo)* **33**, 61 (1992).
6. A. Shima, A. Shimada, T. Itoh and S. Kondo, Fish specific locus test system using the Japanese Medaka (Oryzias latipes) useful for studying radiation-induced germ-cell mutagenesis. In *Proceedings of the 1992 China-Japan Medical Conference on Radiological Biology, Medicine and Protection*, pp. 93–99, 1993.
7. A. Takai, N. Kagawa and K. Fujikawa, Dose- and time-dependent responses for micronucleus induction by X-rays and fast neutrons in gill cells of medaka (Oryzias latipes). *Environ. Mol. Mutagen*. **44**, 100–112 (2004).
8. M. P. Little, Estimates of neutron relative biological effectiveness derived from the Japanese bomb survivors. *Int. J. Radiat. Biol*. **72**, 715–726 (1997).
9. A. M. Kellerer, W. Ruhm and L. Walsh, Indications of the neutron effect contribution in solid cancer data of the A-bomb survivors. *Health Phys*. **90**, 554–564 (2006).
10. B. Gersey, J. Solodak, M. Hada, P. Saganti, R. Wilkins, F. Cucinotta and H. Wu, Micronuclei induction in human fibroblasts exposed *in vitro* to Los Alamos high-energy neutrons. *Adv. Space Res*. **40**, 1754–1757 (2007).
11. B. Gersey, R. Wilkins, H. Huff, R. Dwivedi, B. Takala, J. O. O'Donnell, S. A. Wender and R. C. J. Singleterry, Correlation of neutron dosimetry using a silicon equivalent proportional counter microdosimeter and SRAM SEU cross sections for eight neutron energy spectra. *IEEE Trans. Nucl. Sci*. **50**, 2363–2366 (2003).
12. G. D. Badhwar, H. Huff and R. Wilkins, Alterations in dose and lineal energy spectra under different shieldings in the Los Alamos high-energy neutron field. *Radiat. Res*. **154**, 694–704 (2000).
13. M. Kasahara, K. Naruse, S. Sasaki, Y. Nakatani, W. Qu, B. Ahsan, T. Yamada, Y. Nagayasu, K. Doi and Y. Kohara, The medaka draft genome and insights into vertebrate genome evolution. *Nature* **447**, 714–719 (2007).
14. A. Shima and H. Mitani, Medaka as a research organism: past, present and future. *Mech. Dev*. **121**, 599–604 (2004).
15. J. Wittbrodt, A. Shima and M. Schartl, Medaka – A model organism from the Far East. *Nat. Rev. Genet*. **3**, 53–64 (2002).
16. T. Iwamatsu, Stages of normal development in the medaka Oryzias latipes. *Mech. Dev*. **121**, 605–618 (2004).
17. A. Shima and A. Shimada, Development of a possible nonmammalian test system for radiation-induced germ cell mutagenesis using a fish, the Japanese medaka (Oryzias latipes). *Proc. Natl. Acad. Sci. USA* **88**, 2545–2549 (1991).
18. A. Shima and A. Shimada, Induction of mutations in males of the fish Oryzias latipes at a specific locus after gamma-irradiation. *Mutat. Res*. **198**, 93–98 (1988).
19. A. Shimada, A. Shima, K. Nojima, Y. Seino and R. B. Setlow, Germ cell mutagenesis in medaka fish after exposures to high-energy cosmic ray nuclei: A human model. *Proc. Natl. Acad. Sci. USA* **102**, 6063–6067 (2005).

*20.* K. Ijiri, Development of space-fertilized eggs and formation of primordial germ cells in the embryos of Medaka fish. *Adv. Space Res*. **21**, 1155–1158 (1998).

*21.* C. L. Bladen, M. A. Flowers, K. Miyake, R. H. Podolsky, J. T. Barrett, D. J. Kozlowski and W. S. Dynan, Quantification of ionizing radiation-induced cell death *in situ* in a vertebrate embryo. *Radiat. Res*. **168**, 149–157 (2007).

*22.* C. L. Bladen, W. K. Lam, W. S. Dynan and D. J. Kozlowski, DNA damage response and Ku80 function in the vertebrate embryo. *Nucleic Acids Res*. **33**, 3002–3010 (2005).

*23.* C. L. Bladen, S. Navarre, W. S. Dynan and D. J. Kozlowski, Expression of the Ku70 subunit (XRCC6) and protection from low dose ionizing radiation during zebrafish embryogenesis. *Neurosci. Lett*. **422**, 97–102 (2007).

*24.* P. W. Lisowski, C. D. Bowman, G. J. Russell and S. A. Wender, The Los Alamos National Laboratory Spallation Neutron Sources. *Nucl. Sci. Engin*. **106**, 208–218 (1990).

*25.* S. A. Wender, S. Balestrini, A. Brown, R. C. Haight, C. M. Laymon, T. M. Lee, P. W. Lisowski, W. McCorkle, R. O. Nelson and W. Parker, A fission ionization detector for neutron flux measurements at a spallation source. *Nucl. Instrum. Methods Phys. Res*. **336**, 226–231 (1993).

*26.* B. Gersey, S. Aghara, R. Wilkins, J. Wedeking and R. Dwivedi, Comparison of a tissue equivalent and a silicon equivalent proportional counter microdosimeter to high-energy proton and neutron fields. *IEEE Trans. Nucl. Sci*. **5**, 2276–2281 (2007).

*27.* B. Gersey, S. Aghara, R. Wilkins, J. Wedeking and R. Dwivedi, Comparison of a tissue equivalent proportional counter microdosimeter to high-energy proton and neutron fields. *IEEE Trans. Nucl. Sci*. **54**, 2276–2281 (2007).

*28.* R. M. Zucker, E. S. Hunter and J. M. Rogers, Apoptosis and morphology in mouse embryos by confocal laser scanning microscopy. *Methods* **18**, 473–480 (1999).

*29.* J. Rawlings, S. Pantula and D. Dickey, *Applied Regression Analysis—A Research Tool*. Springer-Verlag, New York, 2001.

*30.* B. Efron and R. J. Tibshirani, *An Introduction to the Bootstrap*. Chapman & Hall, Boca Raton, FL, 1993.

*31.* J. Carpenter and J. Bithell, Bootstrap confidence intervals: when, which, what? A practical guide for medical statisticans. *Stat. Med*. **19**, 1141–1164 (2000).

*32.* Y. Ishida, Y. Ohmachi, Y. Nakata, T. Hiraoka, T. Hamano, S. Fushiki and T. Ogiu, Dose-response and large relative biological effectiveness of fast neutrons with regard to mouse fetal neutron apoptosis. *J. Radiat. Res. (Tokyo)* **47**, 41–47 (2006).

*33.* W. L. Russell and E. M. Kelly, Mutation frequencies in male mice and the estimation of genetic hazards of radiation in men. *Proc. Natl. Acad. Sci. USA* **79**, 542–544 (1982).